

# ChemComm

Accepted Manuscript



This is an *Accepted Manuscript*, which has been through the Royal Society of Chemistry peer review process and has been accepted for publication.

*Accepted Manuscripts* are published online shortly after acceptance, before technical editing, formatting and proof reading. Using this free service, authors can make their results available to the community, in citable form, before we publish the edited article. We will replace this *Accepted Manuscript* with the edited and formatted *Advance Article* as soon as it is available.

You can find more information about *Accepted Manuscripts* in the [Information for Authors](#).

Please note that technical editing may introduce minor changes to the text and/or graphics, which may alter content. The journal's standard [Terms & Conditions](#) and the [Ethical guidelines](#) still apply. In no event shall the Royal Society of Chemistry be held responsible for any errors or omissions in this *Accepted Manuscript* or any consequences arising from the use of any information it contains.

Cite this: DOI: 10.1039/c0xx00000x

www.rsc.org/xxxxxx

## ARTICLE TYPE

## Bifunctional Alkyl Chain Barriers for Efficient Perovskite Solar Cells

Jing Zhang<sup>\*a</sup>, Zhelu Hu<sup>a</sup>, Like Huang<sup>a</sup>, Guoqiang Yue<sup>a</sup>, Jinwang Liu<sup>a</sup>, Xingwei Lu<sup>a</sup>, Ziyang Hu<sup>a</sup>, Minghui Shang<sup>b</sup> and Liyuan Han<sup>c</sup>, Yuejin Zhu<sup>\*a</sup>

Received (in XXX, XXX) Xth XXXXXXXXX 20XX, Accepted Xth XXXXXXXXX 20XX

DOI: 10.1039/b000000x

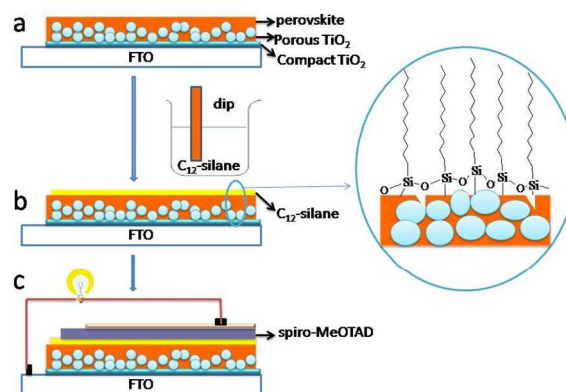
Perovskite solar cells as a hot research topic show great urgency to control the interface. In this work, an insulating alkyl chain layer is self assembled at the perovskite/hole transport material interface, which successfully exhibits dual function to block the electron recombination and resist the moisture at the same time. Improved solar energy conversion efficiency and stability of the device are both achieved.

Solid-state methylammonium lead halide perovskites solar cells are attracting much attention due to their ease of preparation, low cost and high efficiencies<sup>1-4</sup>. Up to now, the perovskite solar cell configuration becomes diverse and fundamentally much different<sup>5</sup>. For example, planar structured perovskite solar cells (without mesoporous TiO<sub>2</sub> layer),<sup>6-8</sup> meso-superstructured<sup>9,10</sup> (with inert mesoporous Al<sub>2</sub>O<sub>3</sub> or ZrO<sub>2</sub> scaffolds) and hole transport material free perovskite solar cells<sup>11</sup>. Though the structure is diverse, the interface lies in all these structures. In general, carriers are created in the perovskite absorber after the absorption of incident photons and travel through a transport pathway including the electron or hole transport layer, the electrodes and each interface in between<sup>12</sup>. Compared with other thin film solar cells, the perovskite solar cell is more prone to surface recombination due to imperfect crystal passivation and undesirable interfacial properties, resulting in fill factor (FF), open circuit voltage (V<sub>oc</sub>) and short-circuit current (J<sub>sc</sub>) losses<sup>13</sup>. Therefore, how to precisely manipulate the interface of perovskite solar cells to maximum the electron and hole separation/collection and minimum the electron recombination decides largely on the real cells' performance.

More recently, there are efforts related to the interface engineering to change the interfacial photoelectrical properties, such as changing the work function of the electrode to a more suitable value<sup>12</sup> or use more efficient electron collection layer<sup>14,15</sup> and blocking layer<sup>5</sup> for efficient charge separation and transportation. Supramolecular halogen bond passivation of surface defect states of perovskite also effectively reduces the interface recombination in the perovskite solar cells<sup>16</sup>.

Despite the evident success of interface engineering to improve the perovskite solar cell performance, the instability problem of perovskite material leaves an open issue for outdoor photovoltaic applications<sup>17</sup>. The instability stems from the CH<sub>3</sub>NH<sub>3</sub>PbI<sub>3</sub> degrades in humid conditions. Replacement of CH<sub>3</sub>NH<sub>3</sub> group with more stable unit under moisture<sup>18</sup> or using hydrophobic hole transport material<sup>19</sup> can effectively alleviate the problem.

Here, a layer with long alkyl chains (dodecyl) is judiciously self assembled on perovskite/TiO<sub>2</sub> nanoparticle surface, which is the first time to use such an electron inactive molecular to perform bifunctionally in perovskite solar cells. On one hand, such alkyl chains function as an electrically insulating barrier, thereby reducing interfacial charge recombination losses in the perovskite solar cells, resulting in much enhanced FF, V<sub>oc</sub> and J<sub>sc</sub>. On the other hand, the interface layer with alkyl chains effectively changes the hydrophilic nature of the perovskite surface to hydrophobic, thus endows the device more resistant of the moisture. It is believed that this bifunctional interface modification can be utilized in other structures of the perovskite solar cells.



Scheme 1. The formation process of the mesoporous perovskite device with C<sub>12</sub>-silane modification.

The formation process of the perovskite device is shown in Scheme 1. The self assembly of monolayer of alkylalkoxysilane molecular is carried out by dip-coating the perovskite/TiO<sub>2</sub> film in dodecyl-trimethoxysilane (C<sub>12</sub>-silane for short) isopropanol solution (the concentration is varied as 0.2, 0.15, 0.1 and 0.05M) for 5 min and baked at 80 ° C to evaporate the solvent. Amphiphilic C<sub>12</sub>-silane has readily hydrolyzable trimethoxysilane groups to hydrolyze or alcoholysis to form silanol, Si-OH (further to form Si-O-Si and Si-OH...HO-Si bonds, the reaction equations are shown in S1 and S2), and a hydrophobic alkyl chain. The alcoholized silanol has Si-OH which is electrophile (Lewis acid), while the I<sup>-</sup> in perovskite is rich in electron pairs (Lewis base)<sup>16</sup>. Therefore, the C<sub>12</sub>-silane can be absorbed on the surface of perovskite by hydrogen bonding of Si-OH with I<sup>-</sup>, leaving the long alkyl chain end group tiltedly stayed outside. With properly

choosing the concentration of the  $C_{12}$ -silane in isopropanol, self-assembled monolayer can be formed and shown in the enlarged view in Scheme 1.

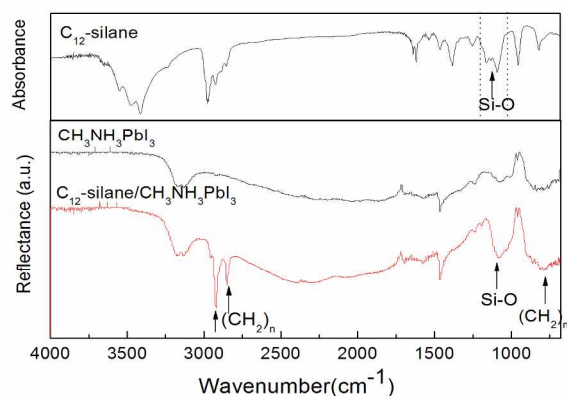


**Figure 1.** Top: FT-IR plot of freshly prepared  $C_{12}$ -silane in isopropanol. Bottom: ATR-FTIR spectra of perovskite  $CH_3NH_3PbI_3$  film and the  $C_{12}$ -silane (0.1M) modified perovskite film ( $C_{12}$ -silane/ $CH_3NH_3PbI_3$ ).

The attenuated total reflectance-Fourier transform infrared (ATR-FTIR) measurement (Figure 1) is used to check the chemical modification of  $C_{12}$ -silane on the surface of perovskite. Pb-I bond is transparent in the IR region; only the organic groups are reflected in IR spectra. The  $-NH_2$  vibration bands ( $3300-3150$ ,  $1535$  and  $1458\text{cm}^{-1}$ ),  $-CH_3$  vibration at  $1230\text{cm}^{-1}$ ,  $-C-N$ -character band at  $1200-1025\text{cm}^{-1}$  can be found in  $CH_3NH_3PbI_3$  spectrum. After interface modification of  $C_{12}$ -silane, new bands clearly appeared in the contrast spectrum as the arrows indicated:  $\gamma$ - $CH_2$  strong stretching bands at  $2920$ ,  $2850\text{cm}^{-1}$  and  $(CH_2)_n$  ( $n > 4$ ) characteristic vibrations at  $720\text{cm}^{-1}$ , which are ascribed to the existence of the  $-C_{12}H_{25}$  alkyl chains<sup>22</sup>; The hydrogen bond of  $Si-OH \cdots I$  cannot directly form a vibration peak in spectra, however, it will affect the  $Si-OH$  vibration. For freshly alcoholized  $C_{12}$ -silane (top of Figure 1), it shows  $Si-O$  and  $Si-O-CH_3$  vibration at  $1185-1035\text{cm}^{-1}$ . When it is assembled on perovskite surface, the vibration band moves to lower frequency region  $1135-1000\text{cm}^{-1}$ , indicating there is an interaction on  $Si-O$ . For the electrophilic property of  $Si-OH$  and the electron pairs on  $I$ , the formation of hydrogen bond  $Si-OH \cdots I$  is thus occurred to influence the  $Si-O$  vibration to lower frequency region. Above changes in the ATR-FTIR spectra indicate the  $C_{12}$ -silane is successfully assembled on the surface of perovskite through hydrogen bonding.

The modified perovskite is further checked by scanning electron microscope (SEM) to examine the surface morphology. As is shown in Figure 2, both of the samples are well crystallized in this experiment with large crystals presented, however, there still existed the holes which uncover the  $TiO_2$  nanocrystalline layer. Compared with the original perovskite film, the  $C_{12}$ -silane modified surface is more compact (inset of Figure 2) which is due to that the  $C_{12}$ -silane might influence the crystallization process of the perovskite during baking. There is a phenomenon should be addressed that the morphology deformation is usually appeared in  $C_{12}$ -silane modified samples during the scanning process. This is actually ascribed to the insulating property of the alkyl chain.

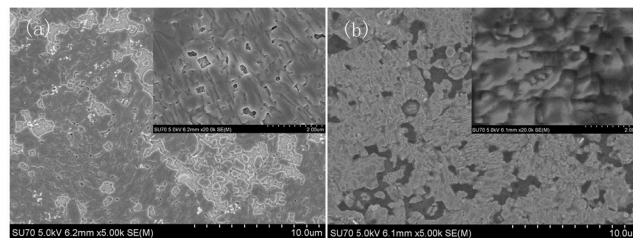


**Figure 2.** The SEM of perovskite film on porous  $TiO_2$ /compact  $TiO_2$ /FTO and the 0.1M  $C_{12}$ -silane solution modified film.

The quality of the as formed perovskite film is critical to the high performance of the device; otherwise, unsuccessful infiltration of perovskite with pin-hole results in low resistance shunting paths, causing electron recombination from the electron transport material (ETM) to the hole transport material (HTM), which is detrimental to the device performance<sup>8,24-26</sup>. In SEM (Figure 2.a) of perovskite film, there are some holes distributed. After  $C_{12}$ -silane modification, the surface of the perovskite appears more homogeneous as is shown in Figure 2.b. Furthermore, the long alkyl chains form a spacer between the perovskite and the HTM (spiro-MeOTAD), which may retard the electron recombination process especially the recombination from the uncovered  $TiO_2$  in the working device, thus the improved performance can be achieved.

Current density versus voltage (J-V) characteristics of the perovskite photovoltaic cells were performed to examine the effects. A batch of more than 35 solar cells were tested and the efficiency distribution is indicated in Figure S1. Most of the cells with  $C_{12}$ -silane modification exhibited superior performances than the original perovskite solar cells. For each  $C_{12}$ -silane concentration, a representative cell is chose with the photovoltaic parameters shown in Table 1.

**Table 1.** The photovoltaic parameters of  $C_{12}$ -silane (different concentrations) modified devices. Light intensity:  $95.6\text{mWcm}^{-2}$ .

concentration	Jsc [ $\text{mAcm}^{-2}$ ]	Voc [V]	FF	Eff [%]
0	18.75	0.908	0.555	9.88
0.05	20.03	0.929	0.666	12.96
0.1	20.23	0.959	0.677	13.74
0.15	19.12	0.942	0.609	11.47
0.2	19.58	0.962	0.555	10.89

The original perovskite solar cell exhibits Jsc of  $18.75\text{mAcm}^{-2}$ , Voc of  $0.908\text{V}$ , FF of  $0.555$  and Eff of  $9.88\%$ . The original device performs ordinarily. By contrast, after the  $C_{12}$ -silane modification, the Voc and FF show solid enhancement, thus the performance is largely improved. The optimum  $C_{12}$ -silane modification (0.1M) results in  $13.74\%$  performance with Jsc of  $20.23\text{mAcm}^{-2}$ , Voc of  $0.959\text{V}$ , FF of  $0.677$ . The current density versus voltage (J-V) curves of these two samples are shown in Figure 3 (a). The increase of FF is due to the enhanced shunt resistance and the reduced series resistance of the cell<sup>27</sup>. In this work, FF exhibits a great improvement from  $0.555$  of the original device to  $0.677$  of  $0.1\text{M}$   $C_{12}$ -silane modified solar cell. The  $C_{12}$ -silane with insulating alkyl chains provides spatial separation between electrons in the perovskite and holes in the solid state hole conductor, increasing the shunt resistance of the device, thus the recombination is retarded and the FF is largely improved. Such insulate or blocking property of the  $C_{12}$ -silane layer in the working cell is illustrated in Figure 3 (b).

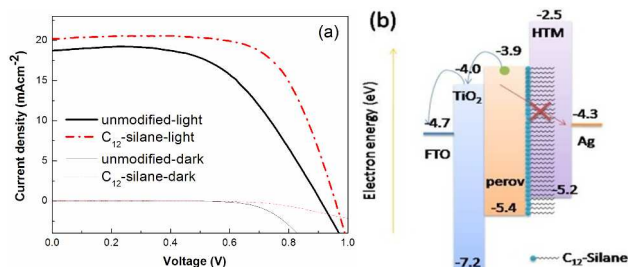


**Figure 3.** (a): The J-V curves of the original perovskite solar cell and the 0.1M C<sub>12</sub>-silane modified device under 95.6mWcm<sup>-2</sup> (AM1.5) and dark; (b): The cell energy level (versus vacuum) diagram of this kind of perovskite solar cell.

The photovoltage will be determined by the difference between the Fermi energy of the perovskite and the HOMO (the highest occupied molecule orbit) energy of the HTM<sup>2</sup>. A change in Voc correlates with the rate of charge carrier extraction and recombination<sup>28</sup>. Here, the improvement of Voc after C<sub>12</sub>-silane modification as is shown in Table 1 is due to the reduced interface recombination by alkyl chain barriers. The higher short-circuit photocurrent densities (Jsc) of the C<sub>12</sub>-silane modified device means high charge separation yields, which is ascribed to the reduced recombination. Too much C<sub>12</sub>-silane content (0.2M) used might influence the hole transfer between the perovskite and the spiro-MeOTAD, which lead to the inferior Jsc compared with the lower C<sub>12</sub>-silane content (Table 1).

The blocking effect of the alkyl chain can be also identified from the dark J-V curves shown in Figure 3 (a). The onset of dark current of C<sub>12</sub>-silane modified device is largely moved to higher bias voltage, which means the extent of recombination is greatly suppressed. (Hysteresis property is shown in Figure S3.)

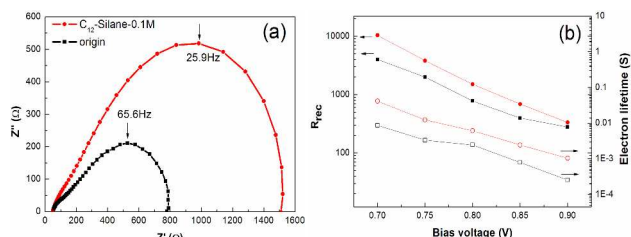


**Figure 4.** The Nyquist plots of original and 0.1M C<sub>12</sub>-silane modified device under dark and bias of 0.8V, (a); the obtained R<sub>rec</sub> and τ versus bias voltage, (b). The lines with black squares represent the original device; the lines with red circles indicate the 0.1M C<sub>12</sub>-silane modified cells.

Electrochemistry impedance spectroscopy (EIS), which recently has been successfully introduced to perovskite solar cell system to monitor the interfacial changes<sup>29,30</sup>, is checked for the two contrast samples. Two arcs are appeared in the Nyquist plots in Figure 4.a: high frequency arc (left part) is ascribed to the contact resistance at the HTM/Ag electrode; while the lower frequency one (right part) is associated with the recombination resistance (R<sub>rec</sub>) and chemical capacitance of the system<sup>31</sup> (equivalent circuit, Figure S2). The R<sub>rec</sub> which is the diameter of the middle frequency arc is related to the recombination of electrons in perovskite/TiO<sub>2</sub> with hole transport layer (HTM). It is clear that the R<sub>rec</sub> is much larger for the 0.1M C<sub>12</sub>-silane modified device under dark at bias of 0.8V compared with the original device, which means that the charge recombination is blocked. It is consistent with the photovoltaic property of the

devices. The electron lifetime τ can be derived from the formula  $\tau = (2\pi f)^{-1}$ , where f is the character frequency. The 0.1M C<sub>12</sub>-silane modified sample shows more prolonged electron lifetime of 6.13mS at 0.8V bias voltage under dark, compared with 2.43mS for the original perovskite solar cell.

Different bias voltages were applied for EIS measurement. The derived R<sub>rec</sub> and τ values plotted with the bias voltage is presented in Figure 4. b. The C<sub>12</sub>-silane modified sample shows higher R<sub>rec</sub> and τ values under all the bias voltage applied, in contrast to the unmodified solar cell. The results strongly support that the insulating/blocking effect of the alkyl chains in C<sub>12</sub>-silane interlayer, thus it prolongs the electron lifetime and facilitates the electron collection.

In fact, interface engineering to form an insulate layer to suppress the electron recombination is not new in dye sensitized solar cells<sup>32</sup>. Here, the same function of the alkyl chains is also achieved in the perovskite solar cells. What is more, it is interesting to notice another phenomenon of the long alkyl chain layer: the contact angles of de-ionized water on the surfaces of C<sub>12</sub>-silane modified and original perovskite films are of great difference.



**Figure 5.** The static contact angle of perovskite film (left) and C<sub>12</sub>-silane/perovskite (right) film with the de-ionized water.

The contact angle of the C<sub>12</sub>-silane modified perovskite film is changed to 86.3°, nearly two times larger than 44.1° of the original film. It indicates the C<sub>12</sub>-silane with hydrophobic alkyl chain effectively changes the hydrophilic property of the perovskite film surface. The modified sample is more hydrophobic than the original one. It is known that CH<sub>3</sub>NH<sub>3</sub>PbI<sub>3</sub> is extremely soluble in water and even in low humidity conditions, which bring instable problem to this device. Even the Li<sup>+</sup> salt in the HTM is hydroscopic which will worsen the instability<sup>19</sup>. Cover the hydrophilic perovskite surface with the hydrophobic chain might change the situation. By checking the XRD of the perovskite film and the device performance change with time, this assumption is verified.

Decomposition of CH<sub>3</sub>NH<sub>3</sub>PbI<sub>3</sub> in moisture will convert to PbI<sub>2</sub> phase<sup>17</sup>. The XRD of perovskite film on glass with and without C<sub>12</sub>-silane modification under a relative humidity level of 40% is presented in Figure 6. (a) and (b). The peaks at 14.06, 28.40, and 43.30° are respectively assigned to the (110), (220), and (330) planes of CH<sub>3</sub>NH<sub>3</sub>PbI<sub>3</sub><sup>9</sup>. It is clear that new phase of PbI<sub>2</sub> is presented in original perovskite film after two days as the star indicated, and the intensity of this peak increases with the time. It indicates that the decomposition is deteriorated with time. By contrast, the C<sub>12</sub>-silane modified perovskite is more stable in the test environment. Such phenomenon is ascribed to the long alkyl chain layer that is resisted of water. The efficiency test results are shown in Figure 6. (c). The efficiency of the original device without the C<sub>12</sub>-silane modification shows steady decrease of the Jsc and the efficiency; while the modified one is more stable with the prolonged time. The unsealed cell with C<sub>12</sub>-silane modification shows increase of Voc and FF within the first 100h.

After 600h in ambient environment, the efficiency keeps 85% of its initial value with Jsc deteriorated.

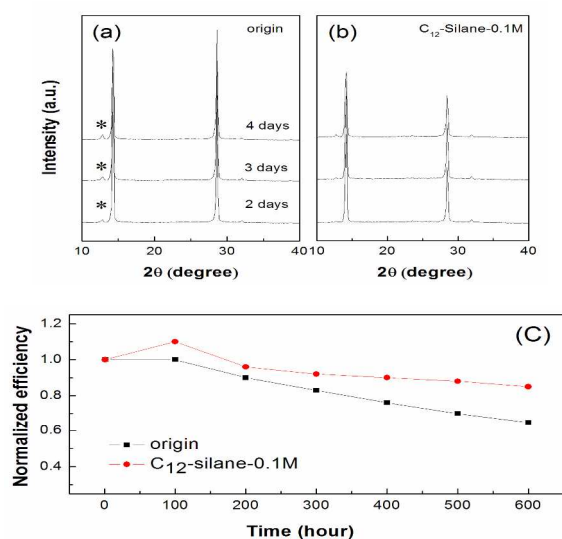


**Figure 6.** The XRD plots of perovskite film (a) and 0.1M C<sub>12</sub>-silane modified perovskite (b) on glass under 40% relative humidity; The normalized efficiency change with time (c), the solar cells are unsealed and the humidity of ambient environment is no more than 45%.

## Conclusions

In conclusion, by a simple dip coating method, an insulating and hydrophobic layer with long alkyl (dodecyl) chain is formed at the perovskite/HTM interface. On one hand, the insulating alkyl chains prohibit the electron back reaction from the TiO<sub>2</sub>/perovskite to HTM, thus effectively enhance the as fabricated solar cell performance with solid increased FF and Voc. Electrochemical characterizations also verify this effect. On the other hand, the hydrophobic alkyl chain layer make the surface of perovskite more resistive to moisture, which renders the device more stable when compared with the unmodified one under ambient environment. The performance of C<sub>12</sub>-silane modification is thus proved to be judicious and bifunctional. Furthermore, it is irradiative that other long alkyl chain silane (C<sub>8</sub>, C<sub>16</sub> or C<sub>20</sub>) may be explored to further optimise the electron transport and the moisture resistant property of the perovskite solar cells.

## ACKNOWLEDGMENT

The authors thank Dr. Qidong Tai and Dr. Jiangwei Feng for their suggestions on this work. We also acknowledge the financial support from the National Natural Science Foundation of China (Grant No. 51302137, 11304170 and 11374168), Qiangjiang Talented Person Project of Zhengjiang (No. QJD1302008) and K.C. Wong Magna Fund in Ningbo University.

## Notes and references

a Department of Microelectronic Science and Engineering, Ningbo University, Zhejiang, 315211, China; E-mail: zhangjing@nbu.edu.cn.  
 b School of Materials Science and Engineering, Ningbo University of Technology, Zhejiang, 315016, China  
 c Photovoltaics Materials Unit, National Institute for Materials Science, Tsukuba, Ibaraki, 305-0047, Japan.

† Electronic Supplementary Information (ESI) available: The reaction equations S1 and S2; The efficiency distribution of the perovskite photovoltaic cells, Figure S1. Figure S2, the equivalent circuit of the Nyquist plot. Figure S3, the hysteresis analyze.

- McGehee MD. *Nat Mater.* 2014;13(9):845-846.
- Kim H S, Lee C R, Im J H, et al. *Scientific reports*, 2012, 2, 591.
- Burschka J, Pellet N, Moon SJ, Humphry-Baker, R.; Gao, P.; Nazeeruddin, M. K.; Grätzel, M.. *Nature.* 2013;499(7458):316-319.
- Cai B, Xing Y, Yang Z, et al. *Energy & Environmental Science*, 2013, 6(5): 1480-1485.
- Chen W, Yongzhen W, Liu J, Qin, C.; Yang, X.; Islam, A.; Cheng, Y.-B.; Han, L. *Energy & Environmental Science.* 2014, 8, 629-640
- Liu M, Johnston MB, Snaith HJ. *Nature.* 2013;501(7467):395-398.
- Chen Q, Zhou H, Hong Z, Luo, S.; Duan, H.-S.; Wang, H.-H.; Liu, Y.; Li, G.; Yang, Y. *Journal of the American Chemical Society.* 2013;136(2):622-625.
- Eperon GE, Burlakov VM, Docampo P, Goriely A, Snaith HJ. *Advanced Functional Materials.* 2014;24(1):151-157.
- Lee MM, Teuscher J, Miyasaka T, Murakami TN, Snaith HJ. *Science.* 2012;338(6107):643-647.
- Bi D, Moon S-J, Haggman L, Boschloo, G.; Yang, L.; Johansson, E. M. J.; Nazeeruddin, M. K.; Grätzel, M.; Hagfeldt, A.. *RSC Advances.* 2013;3(41):18762-18766.
- Xu Y, Shi J, Lv S, et al. *ACS Applied Materials & Interfaces.* 2014;6(8):5651-5656.
- Zhou H, Chen Q, Li G, Luo, S.; Song, T.-b.; Duan, H.-S.; Hong, Z.; You, J.; Liu, Y.; Yang, Y. *Science.* 2014;345(6196):542-546.
- Yamada Y, Nakamura T, Endo M, Wakamiya A, Kanemitsu Y. *Journal of the American Chemical Society.* 2014;136(33):11610-11613.
- Zhong D, Cai B, Wang X, et al. *Nano Energy*, 2015, 11: 409-418.
- Zhu Z, Ma J, Wang Z, et al. *Journal of the American Chemical Society*, 2014, 136(10): 3760-3763.
- Abate A, Saliba M, Hollman DJ, et al. *Nano letters.* 2014.
- Grätzel M. *Nat Mater.* 2014;13(9):838-842.
- Smith IC, Hoke ET, Solis-Ibarra D, McGehee MD, Karunadasa HI. *Angewandte Chemie.* 2014;126(42):11414-11417.
- Zheng L, Chung Y-H, Ma Y, Zhang, L.; Xiao, L.; Chen, Z.; Wang, S.; Qu, B.; Gong, Q. *Chemical Communications.* 2014;50(76):11196-11199.
- Zhang Z, Zakeeruddin SM, O'Regan BC, Humphry-Baker R, Grätzel M. *Journal of Physical Chemistry B.* 2005;109(46):21818-21824.
- Zhang J, Yang Y, Wu SJ, Xu, S.; Zhou, C. H.; Hu, H.; Chen, B. L.; Han, H. W.; Zhao, X. *Z.Electrochimica Acta.* 2008;53(16):5415-5422.
- Zhang J, Yang Y, Wu S, Xu, S.; Zhou, C.; Hu, H.; Chen, B.; Xiong, X.; Sebo, B.; Han, H. *Nanotechnology.* 2008;19(24):245202.
- Cheng Z, Shi B, Gao B, Pang, M.; Wang, S.; Han, Y.; Lin, J. *European Journal of Inorganic Chemistry.* 2005;2005(1):218-223.
- Jeon NJ, Noh JH, Kim YC, Yang WS, Ryu S, Seok SI. *Nat Mater.* 2014;13(9):897-903.
- Xiao M, Huang F, Huang W, Dkhissi, Y.; Zhu, Y.; Etheridge, J.; Gray-Weale, A.; Bach, U.; Cheng, Y.-B.; Spiccia, L. *Angewandte Chemie.* 2014;126(37):10056-10061.
- Wu Y, Islam A, Yang X, Qin, C.; Liu, J.; Zhang, K.; Peng, W.; Han, L. *Energy & Environmental Science.* 2014;7(9):2934-2938.
- Lee J-W, Seol D-J, Cho A-N, Park N-G. *Advanced Materials.* 2014;26(29):4991-4998.
- Im J-H, Jang I-H, Pellet N, Grätzel M, Park N-G. *Nat Nano.* 2014;9(11):927-932.
- Gonzalez-Pedro V, Juarez-Perez EJ, Arsyad W-S, et al. *Nano Letters.* 2014;14(2):888-893.
- Suarez B, Gonzalez-Pedro V, Ripolles TS, Sanchez RS, Otero L, Mora-Sero I. *The Journal of Physical Chemistry Letters.* 2014;5(10):1628-1635.
- Liu D, Yang J, Kelly TL. *Journal of the American Chemical Society.* 2014;136(49):17116-17122.
- Wang P, Zakeeruddin SM, Moser JE, Nazeeruddin MK, Sekiguchi T, Grätzel M. *Nature materials.* 2003;2(6):402-407.